Synthesis, Characterization and Application of Graphene Oxide, Graphene Oxide Quantum Dots and Graphene Guantum Dots in Photoelectrochemical Sensors

Nasrin Ahmadi [1], Ali Nemati [2,*], Mojtaba Bagherzadeh [3]

[1] Department of Materials Engineering, Science and Research Branch, Islamic Azad University, Tehran, Iran
[2] Department of Materials Science & Engineering, Sharif University of Technology, Tehran, Iran
[3] Reactor and Nuclear Safety School, Nuclear Science and Technology Research Institute, 81465-1589, Isfahan, Iran

ARTICLE INFO

Article history:

Received 11 August 2019
Accepted 30 September 2019
Available online 1 November 2019

Keywords:

Graphene
Graphene quantum dots
Photoelectric property
Photoelectrochemical sensor
Dopamine

ABSTRACT

In this study, graphene oxide (GO), graphene oxide quantum dots (GOQD) and graphene quantum dots (GQD) were synthesized by Hummers, hydrothermal and the calcination in argon methods, respectively. Then structure of the samples were characterized by X-ray diffraction, Fourier-transform infrared and Raman spectroscopies and their particle size distribution were investigated by dynamic light scattering. Afterward electrical and photoelectric properties of the samples were studied by electrical conductivity meter and diffuse reflectance and photoluminescence spectroscopies. Finally, the photoelectrochemical sensors were designed to detect dopamine (DA) based on GO, GOQD and GQD modified glassy carbon electrodes (GCE). The results showed that the sample of GO has graphene plates with widest particle size distribution (about 1.3 to 5.7 µm) and the highest electrical conductivity (287.9 µS/cm). On the other, the sample of GQD has narrowest particle size distribution (about 5.3 to 12.8 nm) and the lowest electrical conductivity (165.1 µS/cm). The samples of GOQD and GQD have light absorption throughout range of visible wavelength and therefore have photoelectric behavior better than GO. As a result, in DA detection sensors, the photo response of the GCEs modified with GOQD and GQD is 4 times higher than that of GO modified GCE.

1-Introduction

Graphene, with special properties such as high mechanical flexibility, high specific surface area, unrivaled optical properties, great electrical conductivity and high mobility of charge carriers, has been one of the topics studied materials in recent years [1-3]. Since single layer graphene has a zero band gap and so it doesn't have any photoelectric activity. Therefore, with expanding the number of layers and formation of functional groups and structural defects in graphene, (by formation of graphene oxide or quantization of graphene), it generates a band gap and provides photoelectric activity [4-6]. In some researches, graphene oxide and graphene quantum dots have been used to replace graphene to improve electrical and photoelectric properties [7-9]. Graphene quantum dots demonstrates the features of graphene and carbon quantum dots

* Corresponding author:
E-mail address: nemati@sharif.edu

simultaneously, hence due to its small size and change in band gap, has photoluminescence and semiconductivity properties, and compared to other quantum dots, such as PbS(Se) and CdS(Se), has much less toxicity and much better stability [9-11].

On the other hand, dopamine (DA) determination is substantial, because it as a neurotransmitter has a significant role in diseases such as Parkinson's, schizophrenia and depression [12]. In recent years, different sensors have been designed based on modified electrodes to detect DA [13-14].

In this research, the GO, GOQD and GQD were synthesized and characterized. It is anticipated that all three samples could be useful as electrode modifiers in the photoelectrochemical sensors for determination of dopamine due to their specific electrical and photoelectric properties. Therefore, the performance of modified glassy carbon electrodes with graphene products was compared and evaluated.

2- Experimental procedure

2-1- Materials and equipment

Graphite fine powder extra pure (>99.5%), nitric acid (63%), hydrochloric acid (37%), sulfuric acid (98%), potassium permanganate powder (>99%), hydrogen peroxide (30%) and N-dimethylformamide (DMF) (>99.8%) were purchased from Merck®. The X-ray diffraction(XRD) was used with Cu K_α radiation (λ=0.15418 nm) at a scan rate of 0.05 $2\theta s^{-1}$, (Philips PW3040). Fourier transform infrared spectra (FTIR) were recorded by a FTIR spectrophotometer. (Jasco 6300) and Raman spectra were acquired using a Raman spectrophotometer (FT-Raman 960 with the exciting line at 633 nm of a diode Laser). The particle size distribution of the samples was measured using dynamic light scattering (DLS; Vasco/Corduan technology). Electrical conductivity of samples was investigated by a conductivity meter (Lutron CD-4303) and Ultraviolet-visible light diffuse reflectance spectra (DRS) were performed using a UV-Vis spectrophotometer (Jasco V-670). Photoluminescence (PL) measurements were applied on a fluorescence spectrophotometer (Scino FS-2) using excitation wavelength (λ_{ex}) of 400 nm, and the emission spectrum was scanned over a wavelength range of 300-900 nm.

2-2- Synthesis of graphene oxide, graphene oxide quantum dots and graphene quantum dots

The preparation of graphene oxide was applied using a new method based on the Hammers method [15-16]. For this purpose, 0.5 g of graphite powder was first stirred with sulfuric acid and nitric acid (at a ratio of 3 to 1) for 1 day by magnetic stirrer. Then mixture was washed with deionized water and dried in air for 2 days. Then 0.25 g of dried powder and sulfuric acid (15 mL) were placed on a magnetic stirrer in an ice bath at less than 20 ℃ and then potassium permanganate powder was added to the mixture. After 1 day, deionized water and hydrogen peroxide were added at a ratio of 3 to 1 to the previous compound. Next, the mixture was washed with hydrochloric acid and deionized water several times. Finally, the GO nanoplatelets were prepared after the samples was dried in air for 2 days.

Graphene oxide quantum dots were also fabricated by the hydrothermal method [17], for the synthesis of GOQD, 0.5 g the synthesized GO powder and 5 ml DMF were dissolved into 50 ml deionized water in an ultrasonic bath for 1 hour. Then the suspension was transferred to a 100 ml teflon-sealed autoclave container and heated to 200 ℃ for 12 hours. Next the product was filtered through a 0.22 mm microporous membrane. Finally, the brown suspension was dried in air for 2-3 days and GOQD powder was synthesized.

For the synthesis of graphene quantum dots, the synthesized GOQD powder was calcined and reduced in argon atmosphere in 500 °C for 1 hour to eventually the dark brown powder of GQD was synthesized [17].

2-3- Fabrication of the photoelectrochemical electrodes

In the next step, to design the photoelectrochemical sensors, a glassy carbon electrode (GCE) was polished by using with 0.3 and 0.05 μm alumina powder and then rinsed by sonication in ethanol and deionized water for 5 min. 10 mg the powder (GO, GOQD, GQD) dispersed in 5 ml ethanol and deionized water and then 10 μL of the suspension was coated

onto the GCE surface and dried at room temperature to construction of the GO/GCE, GOQD/GCE and GQD/GCE. The modified GCE was rinsed with water several times prior to use.

2-4- Photoelectrochemical measurements

The photoelectrochemical measurements were performed using PARSTAT 2273 potentiostat/galvanostat and recorded by a conventional tree-electrode system where a GCE, 3 mm in diameter, was used as working electrode, an Ag/AgCl (saturated KCl solution) as a reference and Pt wire as a counter electrode. The photoelectrochemical responses of the modified electrodes were performed in 0.1 M PBS at 0.0 V vs. OCP, under irradiation of a 360 W halogen lamp (GX 6.35 Osram®) within visible wavelength range.

3- Results and discussion

3-1- Characterization of the graphene samples

Figure 1 shows the XRD patterns of GO, GOQD and GQD powders. According to the results the GO contains (001) graphene oxide planes in about 10-degree range and the GOQD and GQD show the broad peak of (002) graphene planes in about 25-degree range [16, 18], the width and the peak shift in these samples is related to the quantization of graphene plates, the disorder and the presence of many functional groups in GOQD and GQD samples [19-20]. The lower peak width of the GQD compared to the GOQD is due to the calcination at high temperature and the crystallite growth of GQD. The average crystallite sizes calculated by using Scherrer equation [21-22], is shown in Table 1.

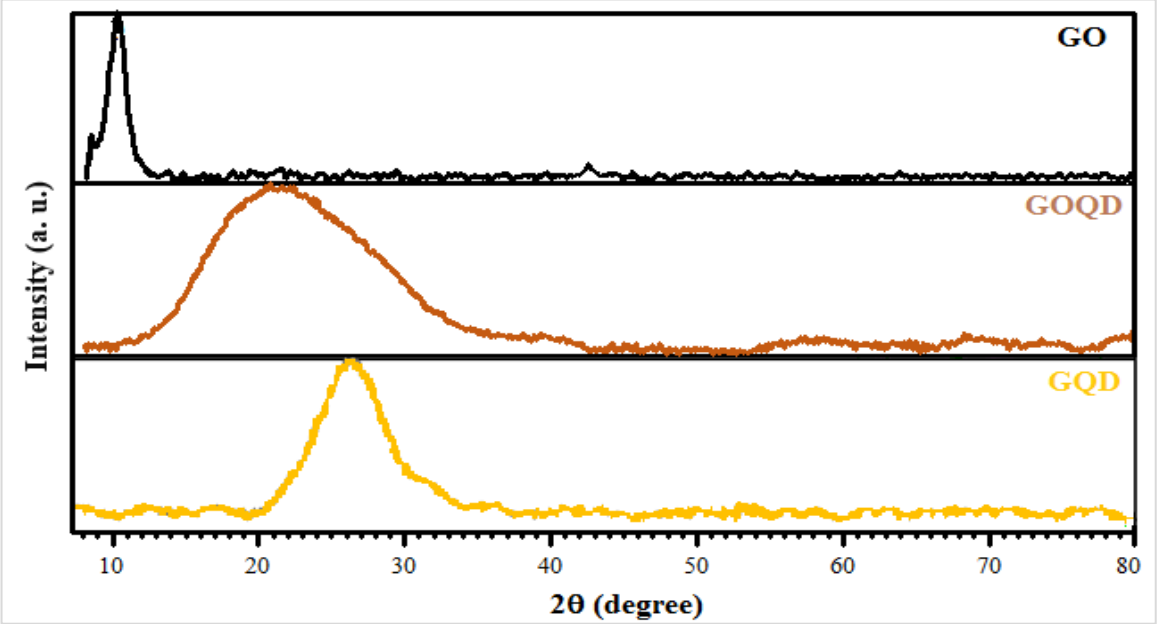

Fig 1. XRD patterns of the GO, GOQD and GQD samples.

Table 1. Crystalline properties of the GO, GOQD and GQD samples.

Sample	2θ (degree)	crystallite size (Å)	FWHM (degree)
GO	10.4	78	1.01
GOQD	22.1	6	13.02
GQD	26.2	16	5.01

The results of FTIR spectroscopy of the samples in Figure 2 also show that the samples have functional groups such as the hydroxyl, carboxyl, carbonyl and epoxy and alkoxy stretching [8, 23-24]. Among the samples, the GOQD sample has the highest diversity and

amount of functional groups due to its quantization and hydrothermal synthesis. On the other hand, the GQD sample has the lowest diversity of functional groups due to calcination, reduction in high temperature and eliminate the most of carbonyl and hydroxyl groups [25-26]. As well as the hydroxyl peak (a board absorption from 3000 to 3700 due to the O-H stretching vibration of the adsorbed water [27].) in this sample has been drastically reduced.

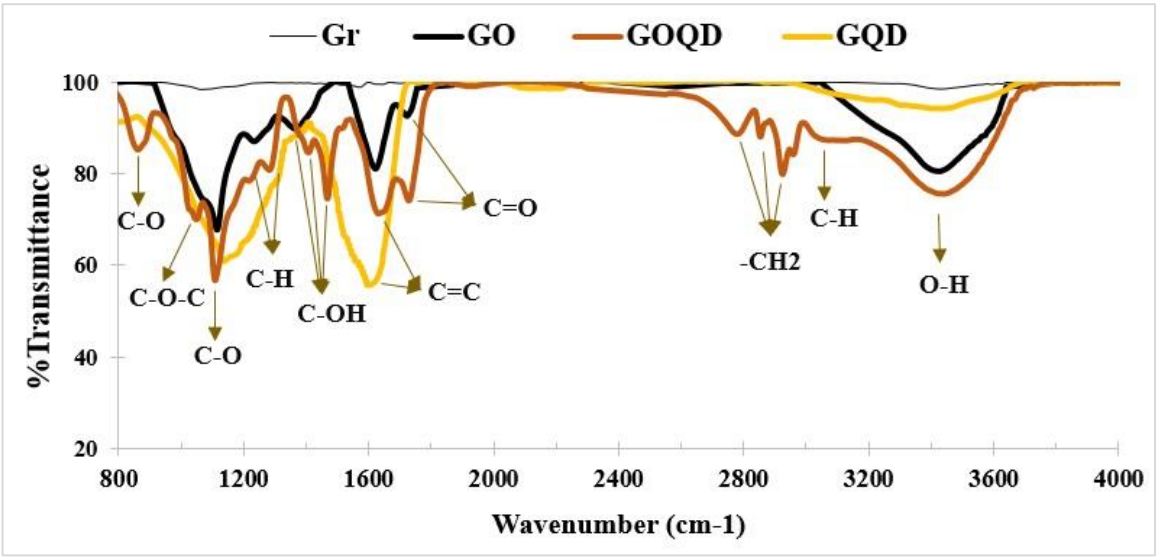

Fig. 2. FTIR spectroscopy of the GO, GOQD and GQD samples.

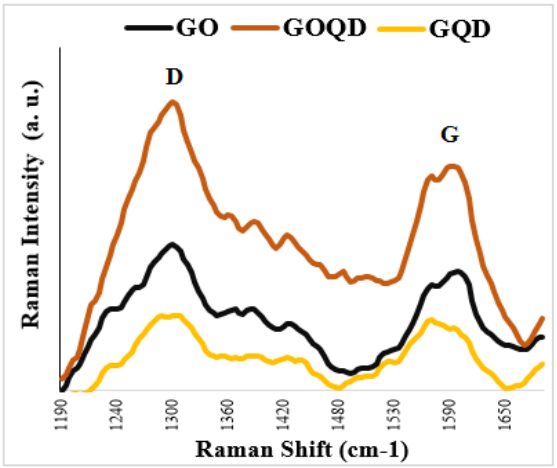

Fig. 3. Raman spectroscopy of the GO, GOQD and GQD samples.

Based on Figure 3 and the results of Raman spectra of the GO, GOQD and GQD samples, two peaks appear at 1290 and 1590 cm^{-1} and are associated with D and G bands, respectively. The D band is related to the edge distortion, defects in graphene or graphene edges and the formation of sp^3 hybridized domains, and the G band is corresponding to the first-order scattering of the E_{2g} mode of sp^2 carbon domains [28-29]. The increase in the intensity of the D to G band intensity ratio (I_D/I_G) indicates an increase in the amount of the disordered phase in the graphene samples [29-30]. Raman spectra of the samples showed that the I_D/I_G ratio of the GO, GOQD and GQD samples are 1.18, 1.29 and 1.06, respectively. The increase in the I_D/I_G ratio of the GOQD compared to the GO is due to the quantization of graphene and the presence of more and more diverse functional groups on the surface and edges of the GOQD [19, 30]. On the other hand, the decrease in the I_D/I_G ratio of the GQD compared to the other samples is due to its calcination at high temperature in argon

atmosphere and the elimination of a number of functional groups [19].

Based on the particle size analysis results by DLS in Figure 4 and Table 2, the GO sample has graphene plates with widest particle size distribution (1.3 to 5.7 µm). On the other, the quantization of graphene plates in the GQD sample is confirmed and this sample has narrowest particle size and the smallest size of particle about 5.3 to 12.8 nm.

3-2- Investigation of the electrical and photoelectric behavior of the graphene samples

Diffuse reflectance spectroscopy results and calculated Kubelka-Munk function, to estimate band gap of the samples [16, 31], are presented in Figure 5a-b and Table 3. The results show that all three samples have the absorption edge throughout range of visible wavelength. The GQD sample has two absorption edges in the UV and visible ranges, while the GOQD and GO samples only have one broad absorption edge in the visible range. On the other hand, the GOQD sample relative to the other samples has higher light absorption in the visible range. The calculated band gaps of the samples by Kubelka-Munk function are summarized in Table 3. As can be seen, the band gaps as about 0.2 and 1.4 eV were estimated for GO and GOQD, respectively, and also GQD has two bandgaps 0.2 and 4.05 eV due to having two light absorption edges, which is related to the quantum dot size variation in the GQD sample.

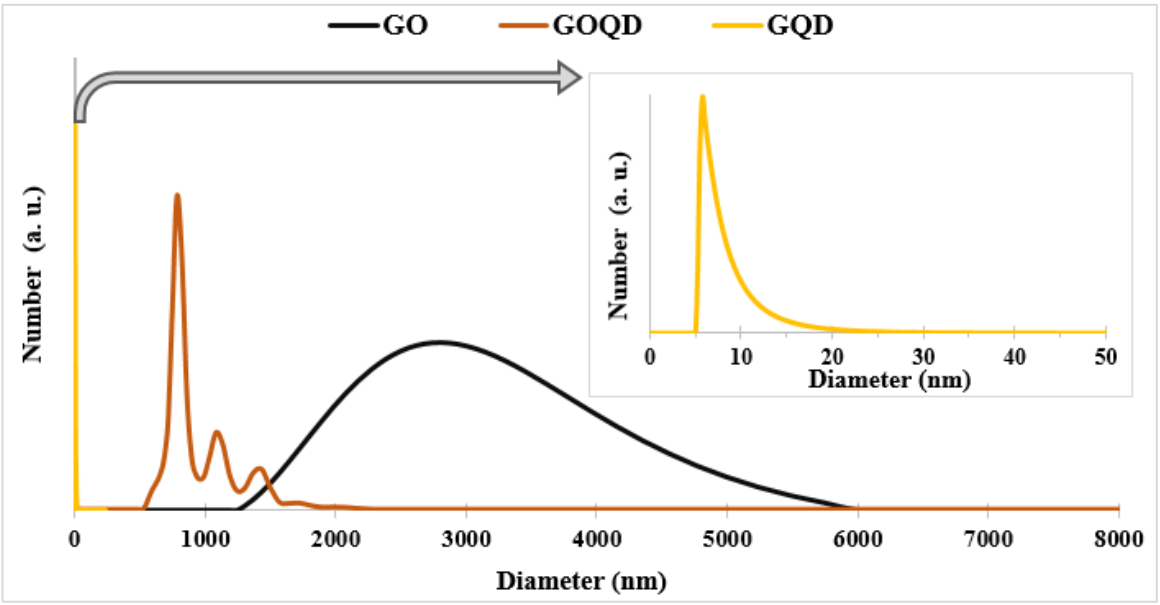

Fig. 4. DLS of the GO, GOQD and GQD samples.

Table 2. Crystalline properties of the GO, GOQD and GQD samples.

Sample	Particle size distribution (nm)	Average particle size (nm)
GO	≅ 1307 - 5740	3005.46
GOQD	≅ 543 - 2076	802.14
GQD	≅ 5.3 – 12.8	7.86

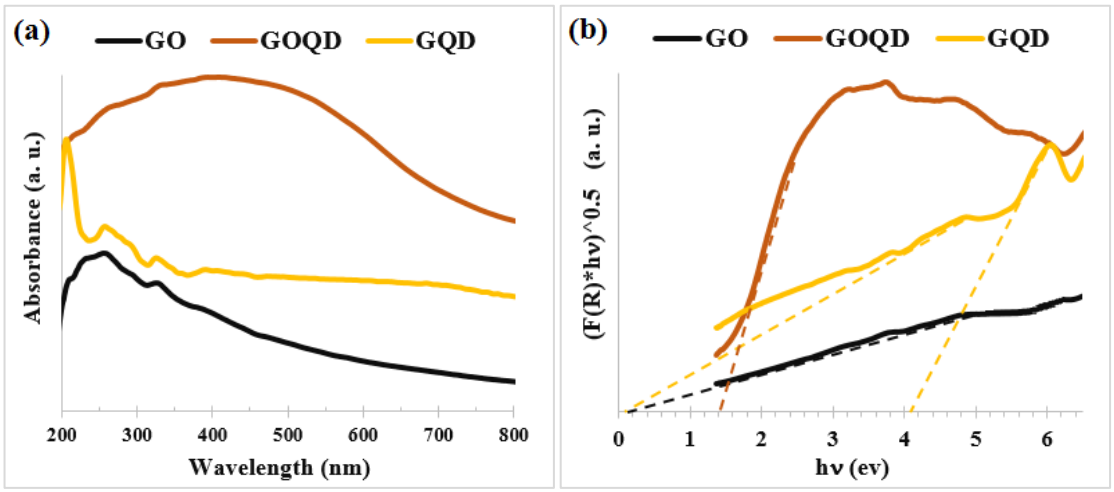

Fig. 5. (a) DRS, (b) Band gap determination of the GO, GOQD and GQD samples.

Table 3. Values of band gap and electrical conductivity of the GO, GOQD and GQD samples.

Sample	Band gap (eV)	Electrical conductivity (μS/cm)
GO	≅ 0.2	≅ 287.9
GOQD	≅ 1.4	≅ 227.8
GQD	≅ 0.2 , 4.05	≅ 165.1

Based on Figure 6, photoluminescence spectroscopy results show, all of the samples exhibit blue, green and red photoluminescence emission peaks at 470, 540 and 830 nm, respectively. In fact, single layer graphene has zero band gap, however, structures of the GO, GOQD and GQD have the band gap which is due to synthesis method, formation of functionalized groups and formation of multi layers graphene [4-6], demonstrated in Figures 2 and 5b. There are similar reports in the literature, as well [32-34]. That might be the main reason why the samples showed photoluminescence activity. In addition, one could observe that photoluminescence emissions of the GOQD and GQD samples are lower than GO sample. But the point to note is that, the band gap of the GO is smaller than the other two, and so the number of photo excited electron-hole pair in it is higher, but it seems the decrease in the photoluminescence emissions of the GOQD and GQD samples occurred due to the quantization of graphene and the trapping of excited electrons by functional groups of the sample and the trapping of excited electrons by functional groups of the samples, that has caused postponement in the recombination rate of photo-induced charge carriers [35-36].

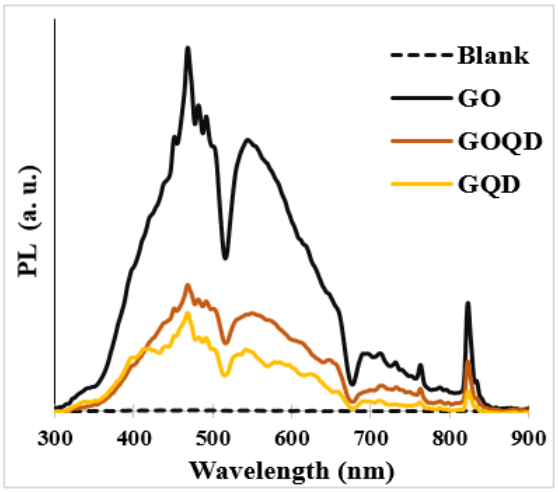

Fig. 6. PL spectra of the GO, GOQD and GQD samples.

According to Table 3, the electrical conductivities of the GO, GOQD and GQD are 287.9, 227.8 and 165.1 (μS/cm), respectively. The GO sample exhibits highest electrical conductivity. In the GOQD and GQD samples, the electrical conductivity is reduced due to the

quantization of graphene plates and the breaking of carbon-carbon bonds.

4- Discussion of the photoelectrochemical sensors

The photoelectrochemical responses of GCE and GQD/GCE in the presence and absence of dopamine were investigated in 0.1 M PBS, pH: 7.4 under visible irradiation and are shown in Figure 7. The photocurrent generated by the GCE is approximately unremarkable. But the photocurrent response of GQD/GCE has been dramatically increased by the addition of DA. Generally, light irradiation induces photo-excited electron-hole pair in the GQD which also recombines a significant part of charge carriers. The electrons then transfer to the electrode. Presence of the DA, as an electron donor, lead to occupy the holes in the valence band of the GQD and prevent recombination of the electron-hole pair. And it causes to increase the number of electrons transmitted during this process [37-38]. In general, the presence of DA increases the number of effectual charge carriers and the photocurrent.

The photoelectrochemical responses of other modified electrodes were recorded and compared with GCE in Figure 8. Under visible light irradiation (at 0.0 V vs. OCP) different photocurrent responses are observed for modified electrodes. The photocurrent generated by the GCE is approximately ignorable. The GO/GCE exhibits photocurrent response due to the small band gap of the GO (≈ 0.2 eV) and excitation of electron-hole pair and the high electrical conductivity of the GO sample (287.9 µS/cm). But the GOQD/GCE and GQD/GCE have higher photocurrent response than GO/GCE (more than 4 times). The observed behaviour in GQD is due to excitation of electron-hole pair under irradiation of visible light in GQD, in addition to electron trapping and preventing the electron-hole pair recombination due to structural defects and surface functional groups on the GQD sample (according to Figures 2 and 3). Furthermore, the increase of photocurrent response recorded by GOQD/GCE compared to GQD/GCE can be due to higher electrical conductivity and more amount of functional groups of the GOQD than the GQD (according to Table 3).

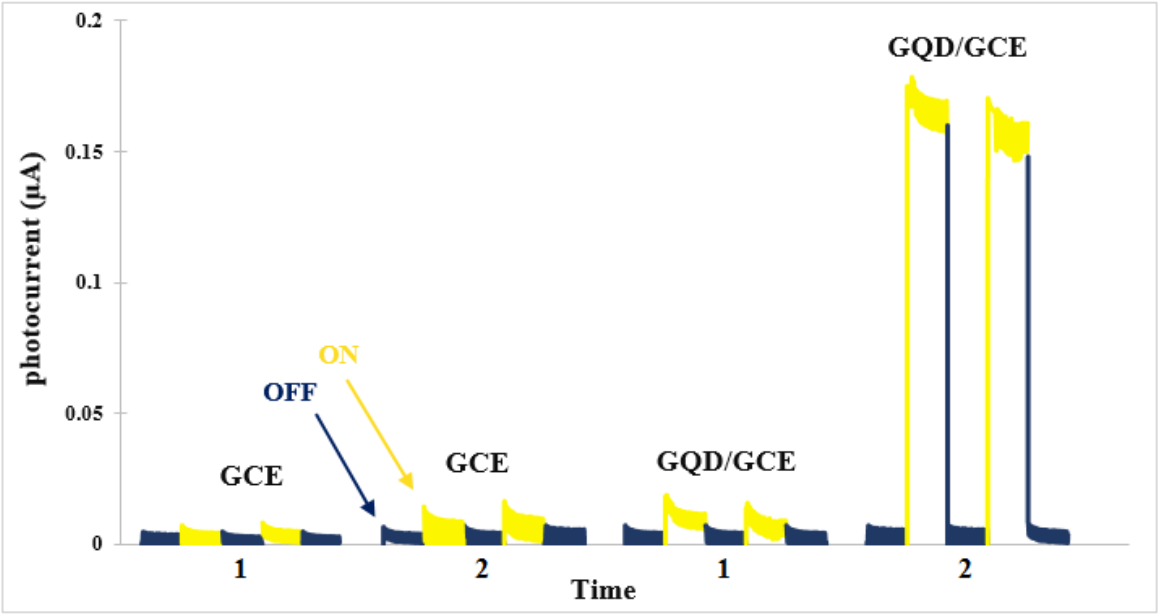

Fig. 7. The photocurrent intensity of the GCE and GQD/GCE in 0.1 M PBS (pH**:** 7.4) without (1) and with (2) 50 µM DA.

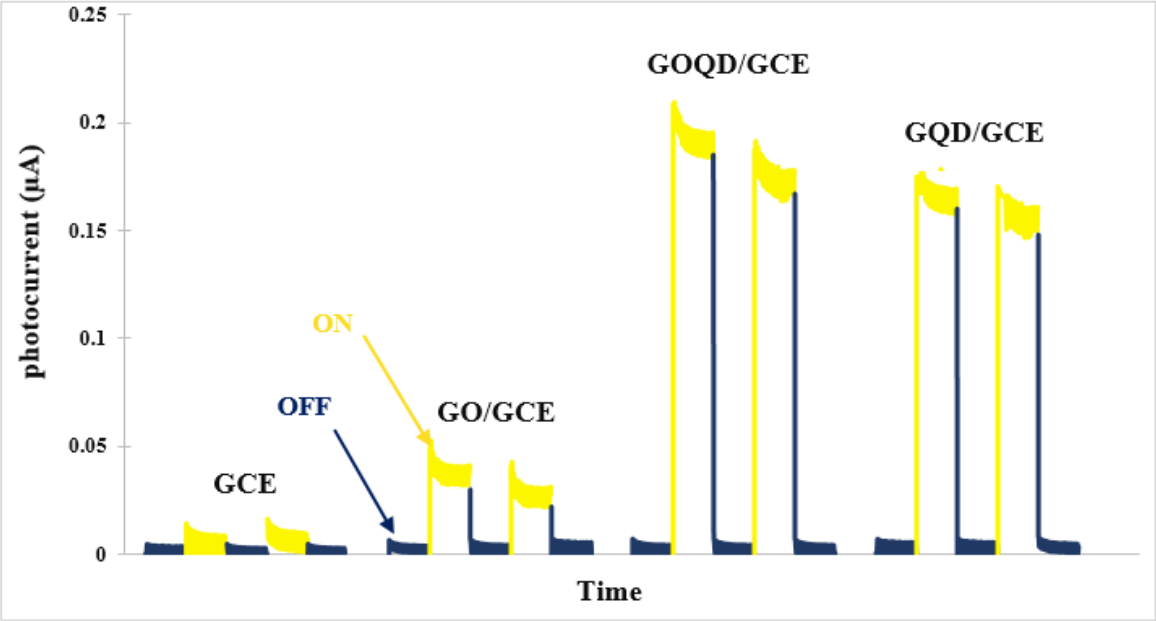

Fig. 8. The photocurrent response of GCE, GO/GCE, GOQD/GCE and GQD/GCE in 0.1 M PBS (pH**:** 7.4) containing 50 µM DA.

5- Conclusions

In this research, the graphene oxide (GO), graphene oxide quantum dots (GOQD) and graphene quantum dots (GQD) were synthesized and characterized. The results show that the GO has graphene plates with particle size distribution about 1 to 6 µm, and the GQD is quantized and has particle size distribution about 5.3 to 12.8 nm. The samples have the light absorption and the widths of absorption edge in the whole of visible light wavelengths. So the specimens have small band gaps in the visible range. In addition, the photoluminescence emission of the GOQD and the GQD are about 60% lower than that of the GO, due to the trapping of excited electron-hole pair by the diverse functional groups of the GOQD and GQD and and decrease of the charge carrier recombination rate. On the other hand, photoelectrochemical responses of the dopamine detection sensors based on GO/GCE, GOQD/GCE and GQD/GCE were investigated and compared. Modified electrodes have shown a better photo response to dopamine detection than GCE due to the electrical conductivity and photoelectric properties of graphene modifiers. Based on the investigations, PEC response of GOQD/GCE is more than 4 times of PEC response of GO/GCE due to the structural defects and surface functional groups on the GOQD sample as electron trapping and preventing the electron-hole pair recombination.

References:

[1] M. Bagherzadeh, A. Farahbakhsh, Surface Functionalization of Graphene, in: Graphene Materials, John Wiley & Sons, Inc., 2015, p. 25-65.

[2] D.R. Cooper, B. D'Anjou, N. Ghattamaneni, B. Harack, M. Hilke, A. Horth, N. Majlis, M. Massicotte, L. Vandsburger, E. Whiteway, V. Yu, "Experimental Review of Graphene", ISRN Condens. Matter Phys., Vol. 2012, 2012, pp. 501686.

[3] J.S. Murray, Z.P.I. Shields, P. Lane, L. Macaveiu, F.A. Bulat, "The average local ionization energy as a tool for identifying reactive sites on defect-containing model graphene systems", J. Mol. Model., Vol. 19, 2013, pp. 2825-2833.

[4] M. Terrones, A.R. Botello-Méndez, J. Campos-Delgado, F. López-Urías, Y.I. Vega-Cantú, F.J. Rodríguez-Macías, A.L. Elías, E. Muñoz-Sandoval, A.G. Cano-Márquez, J.-C. Charlier, H. Terrones, "Graphene and graphite nanoribbons: Morphology, properties, synthesis, defects and applications", Nano Today, Vol. 5, 2010, pp. 351-372.

[5] Z. Sun, H. Chang, "Graphene and Graphene-like Two-Dimensional Materials in

Photodetection: Mechanisms and Methodology", ACS Nano, Vol. 8, 2014, pp. 4133-4156.
[6] R. Garg, N. Dutta, N. Choudhury, "Work Function Engineering of Graphene", Nanomaterials, Vol. 4, 2014, pp. 267-300.
[7] M. Bagherzadeh, Z.S. Ghahfarokhi, E.G. Yazdi, "Electrochemical and surface evaluation of the anti-corrosion properties of reduced graphene oxide", RSC Adv., Vol. 6, 2016, pp. 22007-22015.
[8] W. Zhang, Y. Liu, X. Meng, T. Ding, Y. Xu, H. Xu, Y. Ren, B. Liu, J. Huang, J. Yang, X. Fang, "Graphenol defects induced blue emission enhancement in chemically reduced graphene quantum dots", Phys. Chem. Chem. Phys., Vol. 17, 2015, pp. 22361-22366.
[9] M. Bacon, S.J. Bradley, T. Nann, "Graphene Quantum Dots", Part. Part. Syst. Charact., Vol. 31, 2014, pp. 415-428.
[10] A.D. Güçlü, P. Potasz, M. Korkusinski, P. Hawrylak, Introduction. In: Graphene Quantum Dots, NanoScience and Technology, Springer Berlin Heidelberg, 2014, p. 1.
[11] N. Hashemzadeh, M. Hasanzadeh, N. Shadjou, J. Eivazi-Ziaei, M. Khoubnasabjafari, A. Jouyban, "Graphene quantum dot modified glassy carbon electrode for the determination of doxorubicin hydrochloride in human plasma", J. Pharm. Anal., Vol. 6, 2016, pp. 235-241.
[12] R.K. Shervedani, M. Bagherzadeh, S.A. Mozaffari, "Determination of dopamine in the presence of high concentration of ascorbic acid by using gold cysteamine self-assembled monolayers as a nanosensor", Sens. Actuators, B, Vol. 115, 2006, pp. 614-621.
[13] A. Azzouz, K.Y. Goud, N. Raza, E. Ballesteros, S.E. Lee, J. Hong, A. Deep, K.H. Kim, "Nanomaterial-based electrochemical sensors for the detection of neurochemicals in biological matrices", TrAC, Trends Anal. Chem., Vol. 110, 2019, pp. 15-34.
[14] Y. Li, Z. Li, W. Ye, S. Zhao, Q. Yang, S. Ma, G. Xiao, G. Liu, Y. Wang, Z. Yue, "Gold nanorods and graphene oxide enhanced BSA-$AgInS_2$ quantum dot-based photoelectrochemical sensors for detection of dopamine", Electrochim. Acta, Vol. 295, 2019, pp. 1006-1016.
[15] D. Marcano, D. Kosynkin, J. Berlin, A. Sinitskii, Z. Sun, A. Slesarev, L. B Alemany, W. Lu, J. Tour, "Improved synthesis of graphene oxide", ACS Nano, Vol. 4, 2010, pp. 4806-4814.
[16] N. Ahmadi, A. Nemati, M. Bagherzadeh, "Synthesis and properties of Ce-doped TiO_2-reduced graphene oxide nanocomposite", J. Alloys Compd., Vol. 742, 2018, pp. 986-995.
[17] Y. Yu, J. Ren, M. Meng, "Photocatalytic hydrogen evolution on graphene quantum dots anchored TiO_2 nanotubes-array", Int. J. Hydrogen Energy, Vol. 38, 2013, pp. 12266-12272.
[18] W.D. Yang, Y.R. Li, Y.C. Lee, "Synthesis of r-GO/TiO_2 composites via the UV-assisted photocatalytic reduction of graphene oxide", Appl. Surf. Sci., 380, 2016, pp. 249-256.
[19] S. Sarkar, D. Gandla, Y. Venkatesh, P.R. Bangal, S. Ghosh, Y. Yangd, S. Misrae, "Graphene quantum dots from graphite by liquid exfoliation showing excitation-independent emission, fluorescence upconversion and delayed fluorescence", Phys. Chem. Chem. Phys., Vol. 18, 2016, pp. 21278-21287.
[20] Z. Huang, Y. Shen, Y. Li, W. Zheng, Y. Xue, C. Qin, B. Zhang, J. Haoa, W. Feng, "Facile synthesis of analogous graphene quantum dots with sp^2 hybridized carbon atom dominant structures and their photovoltaic application", Nanoscale, Vol. 6, 2014, pp. 13043-13052.
[21] L. Luo, T. Li, X. Ran, P. Wang, L. Guo, "Probing photocatalytic characteristics of Sb-Doped TiO_2 under visible light irradiation", J. Nanomater., Vol. 2014, 2014, pp. 1-6.
[22] N. Ahmadi, A. Nemati, M. Solati-Hashjin, "Synthesis and characterization of co-doped TiO_2 thin films on glass-ceramic", Mater. Sci. Semicond. Process., Vol. 26, 2014, pp. 41–48.
[23] S. Huang, L. Song, Z. Xiao, Y. Hu, M. Peng, J. Li, X. Zheng, B. Wu, C. Yuan, "Graphene quantum dot-decorated mesoporous silica nanoparticles for high aspirin loading capacity and its pH-triggered release", Anal. Methods, Vol. 8, 2016, pp. 2561-2567.
[24] M. Bagherzadeh, M. Heydari, "Electrochemical detection of dopamine based on pre-concentration by graphene nanosheets", Analyst, Vol. 138, 2013, pp. 6044-6051.
[25] K. Muthoosamy, R.G. Bai, I.B. Abubakar, S.M. Sudheer, H.N. Lim, H.-S. Loh, N.M. Huang, C.H. Chia, S. Manickam, "Exceedingly biocompatible and thin-layered reduced graphene oxide nanosheets using an eco-

friendly mushroom extract strategy", Int. J. Nanomed., Vol. 10, 2015, pp. 1505-1519.
[26] H. Liu, L. Zhang, Y. Guo, C. Cheng, L. Yang, L. Jiang, G. Yu, W. Hu, Y. Liu, D. Zhu, "Reduction of graphene oxide to highly conductive graphene by Lawesson's reagent and its electrical applications", J. Mater. Chem. C, Vol. 1, 2013, pp. 3104-3109.
[27] X. Liu, R. Yan, J. Zhu, J. Zhang, X. Liu, "Growing TiO_2 nanotubes on graphene nanoplatelets and applying the nanonanocomposite as scaffold of electrochemical tyrosinase biosensor", Sens. Actuators, B, Vol. 209, 2015, pp. 328-335.
[28] L. Bokobza, J.L. Bruneel, M. Couzi, "Raman Spectra of Carbon-Based Materials (from Graphite to Carbon Black) and of Some Silicone Composites", C, Vol. 1, 2015, pp. 77-94.
[29] M. S. Dresselhaus, A. Jorio, A.G. Souza Filho, R. Satio, "Defect characterization in graphene and carbon nanotubes using Raman spectroscopy", Phil. Trans. R. Soc. A, Vol. 368, 2010, pp. 5355–5377.
[30] P. Roy, A.P. Periasamy, C.Y. Lin, G.M. Her, W.J. Chiu, C.L. Li, C.L. Shu, C. Huang, C.T. Liang, H. T. Chang, "Photoluminescent graphene quantum dots for in vivo imaging of apoptotic cells", Nanoscale, Vol. 7, 2015, pp. 2504-2510.
[31] R. López, R. Gómez, "Band-gap energy estimation from diffuse reflectance measurements on sol–gel and commercial TiO_2: a comparative study", J. Sol-Gel Sci. Technol., Vol. 61, 2011, pp. 1-7.
[32] G. Eda, Y.Y. Lin, C. Mattevi, H. Yamaguchi, H.A. Chen, I.S. Chen, C.W. Chen, M. Chhowalla, "Blue Photoluminescence from Chemically Derived Graphene Oxide", Adv. Mater., Vol. 22, 2010, pp. 505-509.
[33] M. Orlita, M. Potemski, "Dirac electronic states in graphene systems: optical spectroscopy studies", Semicond. Sci. Technol., Vol. 25, 2010, pp. 063001.
[34] S.K. Pal, "Versatile photoluminescence from graphene and its derivatives", Carbon, Vol. 88, 2015, pp. 86-112.
[35] S. Gayathri, M. Kottaisamy, V. Ramakrishnan, "Facile microwave-assisted synthesis of titanium dioxide decorated graphene nanocomposite for photodegradation of organic dyes", AIP Adv., Vol. 5, 2015, pp. 127112.
[36] G.S.H. Thien, F.S. Omar, N.I.S.A. Blya, W.S. Chiu, H.N. Lim, R. Yousefi, F.J. Sheini, N.M. Huang, "Improved Synthesis of Reduced Graphene Oxide-Titanium Dioxide Composite with Highly Exposed 001 Facets and Its Photoelectrochemical Response", Int. J. Photoenergy, Vol. 2014, 2014, pp. 650583.
[37] X. Hun, S. Wang, S. Mei, H. Qin, H. Zhang, X. Luo, "Photoelectrochemical dopamine sensor based on a gold electrode modified with SnSe nanosheets", Microchim. Acta, Vol. 184, 2017, pp. 3333-3338.
[38] H. Ye, H. Wang, B. Zhang, F. Zhao, B. Zeng, "Tremella-like $ZnIn_2S_4$/graphene composite based photoelectrochemical sensor for sensitive detection of dopamine", Talanta, Vol. 186, 2018, pp. 459-466.